Journal Homepage: - www.journalijar.com

INTERNATIONAL JOURNAL OF ADVANCED RESEARCH (IJAR)

ISSN NO. 2320-5407

Article DOI: 10.21474/IJAR01/14011
DOI URL: http://dx.doi.org/10.21474/IJAR01/14011

RESEARCH ARTICLE

SIMULATION OF THE OKRA DRYING PROCESS IN A SOLAR TOWER DRYER

Germain Wende Pouiré Ouedraogo[1,3], Boureima Kaboré[2,3], Nebon Bado[3], Vincent Zoma[3], Sié Kam[3] and Dieudonné Joseph Bathiébo[3]

1. Higher School of Engineering (ESI), University of Fada N'Gourma, Fada N'Gourma, Burkina Faso.
2. Laboratory of Research in Energetic and Space Meteorology, University Norbert ZONGO, Koudougou, Burkina Faso.
3. Laboratory of Renewable Thermal Energies, University Joseph KI-ZERBO, Ouagadougou, Burkina Faso.

Manuscript Info

Manuscript History
Received: 05 November 2021
Final Accepted: 09 December 2021
Published: January 2022

Key words:-
Drying Air, Drying, Solar Tower Dryer, Okra, Fortran

Abstract

This work presents the simulation of the drying air flow in a solar tower dryer as well as the okra drying process with FORTRAN software. The explicit Euler method was used for solving the heat transfer and mass transfer equations. The heat transfer equations reflect the flow of hot air from the manifold and directed into the drying chamber, while the mass transfer equations reflect the removal of moisture from the fresh product through the exchange of heat. This simulation gives an idea of the heat input received by the air after it enters the dryer manifold and then its action on the product to be dried. This is how we were able to determine the different variations in air temperature within the dryer, the variations in temperature and humidity of the product as well as the drying time of the product.

Introduction:-

Sun drying is one of the most widely used conservation methods for agricultural products in sub-Saharan Africa, mainly in Burkina Faso ([1]; [2]; [3]). It leads to loss of moisture, reduction in weight and size of the product in order to ensure its storage and transport [4]. Studies have determined the recommended drying temperatures and water content for different types of products, which prevent the growth of bacteria and the loss of certain nutrients [5].

Several solar dryers have been designed for this purpose to improve traditional drying, drying time, hygiene and conservation of the majority of the nutrients contained in the products ([1]; [5]; [6]; [7]; [8]; [9]; [10]).

As part of their work, authors have modeled the drying process to determine the drying curves ([11]; [12]; [13]).

The objective of this work is to simulate the drying of okra cut into a cylindrical shape. It will simulate the temperature profile of the product, the relative humidity of the air and the drying kinetics by introducing the variation in the water content test of okra in the computer code.

Description of the solar tower dryer

The solar tower dryer consists of the collector and the drying chamber. This indirect solar dryer works by natural convection and allows a certain amount of water to be extracted from the product in order to obtain a good quality

Corresponding Author:- Boureima Kabore
Address:- Laboratory of Research in Energetic and Space Meteorology, University Norbert Zongo, Koudougou, Burkina Faso.

dry product. Air is heated in the collector by greenhouse effect and then passed into the drying chamber where the products are spread out on racks. This is where the hot drying air pulls water molecules from the products and continues its way out of the dryer. Figure 1 illustrates the solar tower dryer.

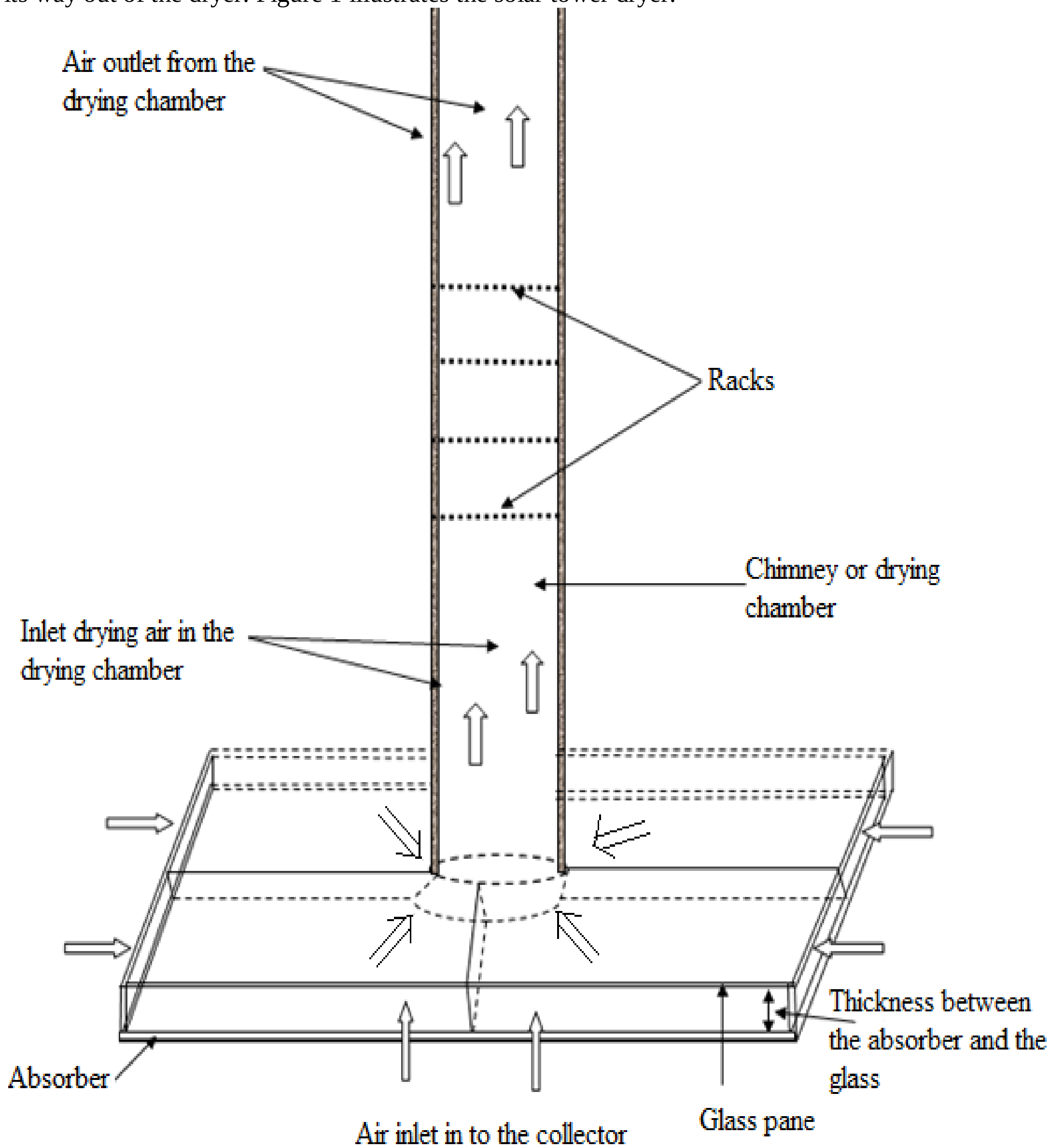

Figure 1:- Solar tower dryer [10].

Coupled heat and mass transfer equations in the drying chamber

Okra to be dried subjected to the flow of hot air from the collector will give out water to the drying air as it passes through the racks containing said product. So okra receives heat from the hot air stream which in turn is the site of mass transfer. Suppose the drying chamber is cut into a number of fictitious slices in the direction of flow, and the okra slices are cylindrical in shape. The volume considered is delimited around a drying rack including the products and the walls of the chamber. This process, shown diagrammatically in Figure 2, describes the various transfers.

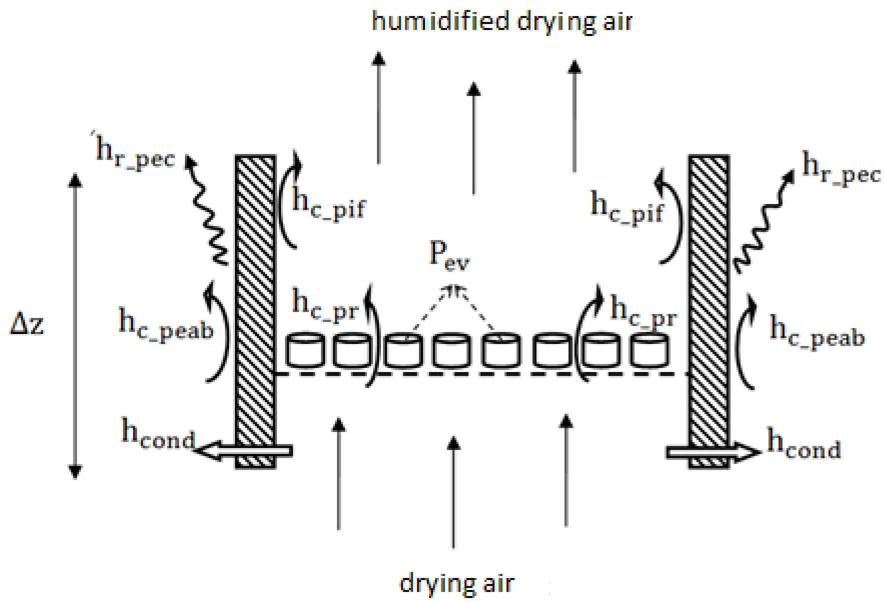

Figure 2:- Heat and mass exchanges at the level of a dryer rack.

This figure 2 allows us to write all the heat and mass exchange equations at the level of a rack of the drying chamber.

Thermal balance on the outer wall (pe)

$$m_{pe} C_{ppe} \frac{\partial T_{pe}}{\partial t} = -S_{pe} h_{c\_peab} \left(T_{pe} - T_{ab}\right) - S_{pe} h_{c\_pec} \left(T_{pe} - T_{c}\right) + S_{pe} h_{cond} \left(T_{pi} - T_{pe}\right) \quad (1)$$

a) *2.2) Heat balance on the inner wall (ft)*

b) $$\boldsymbol{m_{pi} C_{ppi} \frac{\partial T_{pi}}{\partial t} = S_{pi} h_{c\_pif} \left(T_f - T_{pi}\right) - S_{pi} h_{cond} \left(T_{pi} - T_{pe}\right)} \quad (2)$$

c) *2.3) Heat and mass balance of the drying air*

$$\dot{m}_f C_{pf} \Delta z \frac{\partial T_f}{\partial z} = -S_{pr} h_{c\_pr} \left(T_f - T_{pr}\right) - S_{pi} h_{c\_pif} \left(T_f - T_{pi}\right) \quad (3)$$

d) *2.4) Thermal and mass balance on the product (pr)*

e) $$\boldsymbol{m_{pr} C_{ppr} \frac{\partial T_{pr}}{\partial t} = S_{pr} h_{c\_pr} \left(T_f - T_{pr}\right) - P_{ev}} \quad (4)$$

Where the power of evaporation has for expression:

$$P_{ev} = m_s \left(-\frac{d\chi}{dt}\right) L_v \quad (5)$$

With m_s: the dry mass of the Okra (kg)

$\left(-\frac{d\chi}{dt}\right)$: Okra drying speed ($kg_{water}.kg^{-1}_{dry}.s^{-1}$)

The heat of vaporization of the okra water ($J.kg^{-1}_{water}$) is given by Michel Daguenet in 1985 [14]:

$$L_v = 4186{,}5(597 - 0{,}56 T_{pr}) \quad (6)$$

The okra mass calorific capacity is given by R.A Okedun in 2007 [15]:

$$C_{ppr} = -2{,}7663 + 1{,}5448\chi - 0{,}0374\chi^2 + 0{,}0003\chi^3 \quad (7)$$

χ: The water content of the okra.

Resolution method and flowchart

The resolution method used is that of Euler explicit. The diagram is explicit because knowing the initial values, we can explicitly determine the values at the next time. That is to say that it calculates the approximate value in time tj+1 by simple matrix product with the approximate value at tj time. In particular in this method, no matrix reversal or linear system resolution is necessary for the calculation. The flowchart of the drying process is presented in Figure 3.

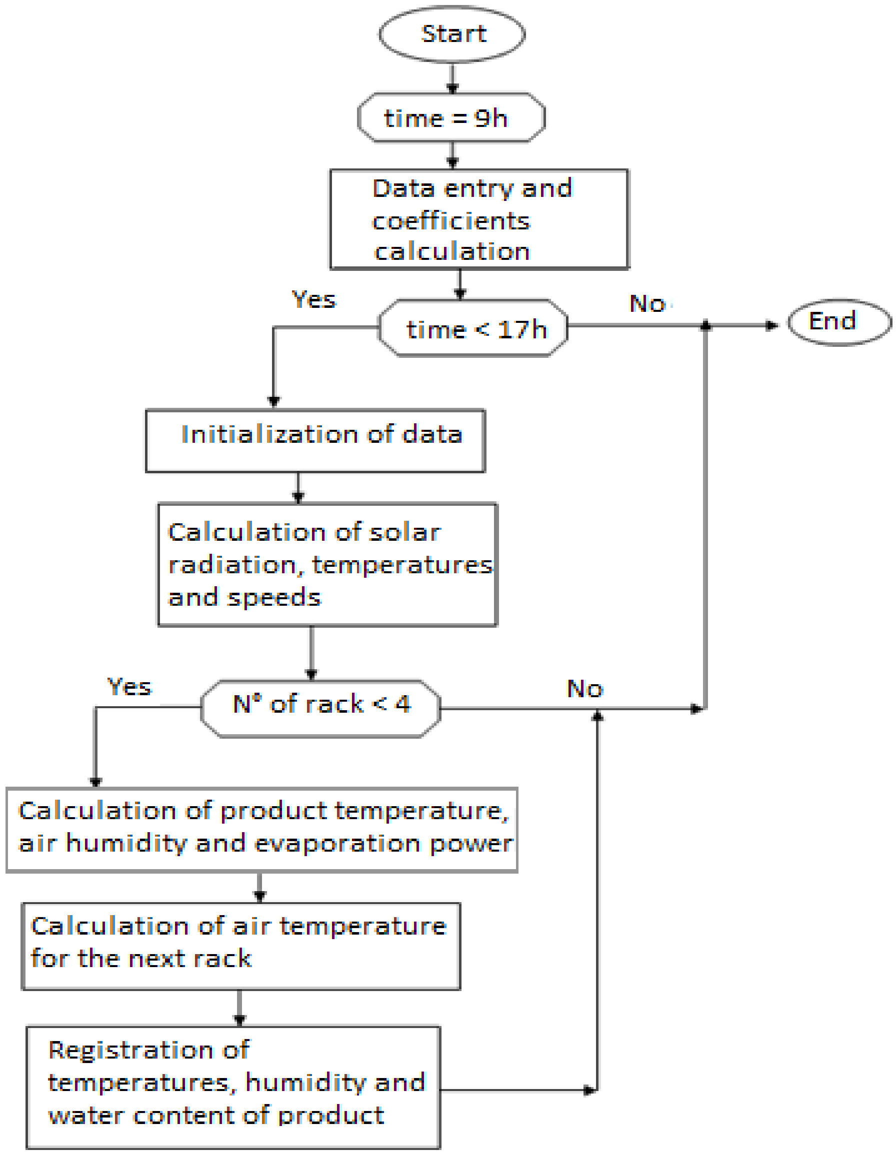

Figure 3:- Organization chart of the drying process.

Results:-

The simulation of the drying okra drying in cylindrical shaped allowed us to have the kinetics of drying, the temperature of the okra slices arranged on each rack and the relative humidity of the air drying in the chamber to dry. The variation of the drying speed was obtained thanks to the introduction of the data of the variation of the exercise water content of the okra into the calculation code.

Okra temperature at the level of the racks

Figure 4 gives the temperature variation of the okra slices placed on each rack according to the drying time.

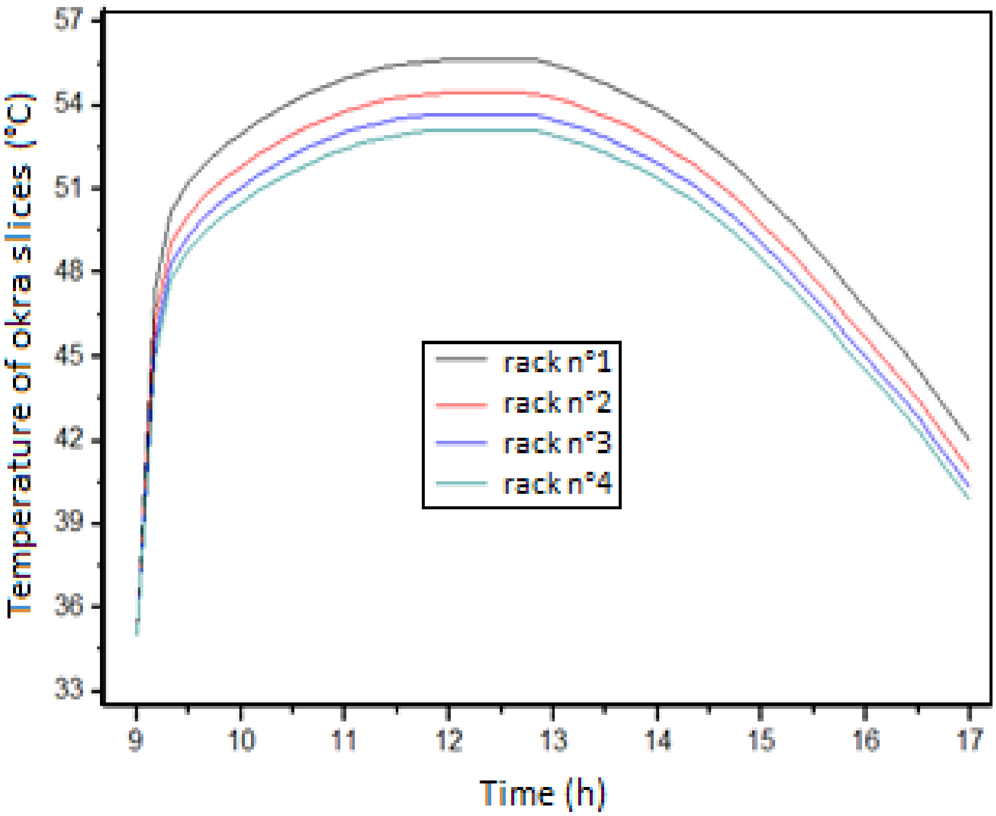

Figure 4:- Variation of the temperature of the okra slice as a function of time.

We observe that the temperature of the Gombo slice placed on the n˚1 rack is greater than those of the slices arranged on the other ransacles in ascending order of the rack position. These temperatures are almost the same or a 1.17˚C gap between the Gombo temperature of the n˚1 Clay and the Gombo of the n˚2 Range. This difference decreases up to 0.57˚C between the Gombo temperature of the n˚3 Clay and that of the Gombo of the n˚4 Clay. B. Dianda in 2016 during the simulation of the convective drying of the tomato slices, asserted that the temperatures of the tomato slices at the level of the different rays are substantially equal, a difference of 0.05˚C [16]. The gombo slices arranged on the racks, warm up as and measurements thanks to the drying air from the collector whose temperature depends on the variation of solar radiation. From 9h to 12h, the temperatures of the gombo slices vary and reach maximum temperatures of 55.63˚c; 54.45˚C; 53.68˚C and 53.11˚C respectively at the level of the N˚1 rack at the N˚4 ramble. This temperature growth indicates that this is the temperature phase of the product where the product warms up to a maximum. These temperature values remain constant between 12h and 12h 40min. It is the evaporation phase of the water at constant speed [14]. Suite these temperatures decrease and reach at 17 hours of the respective temperatures of 41.95˚C; 40.92˚C; 40.28˚C and 39.85˚C. These results were obtained by considering the initial temperature of the Gombo equal to the ambient temperature of the drying day, estimated at 35˚C.

Relative humidity of drying air through the rams

The variation of the theoretical relative humidity of the drying air passing through each rack is given in Figure 5.

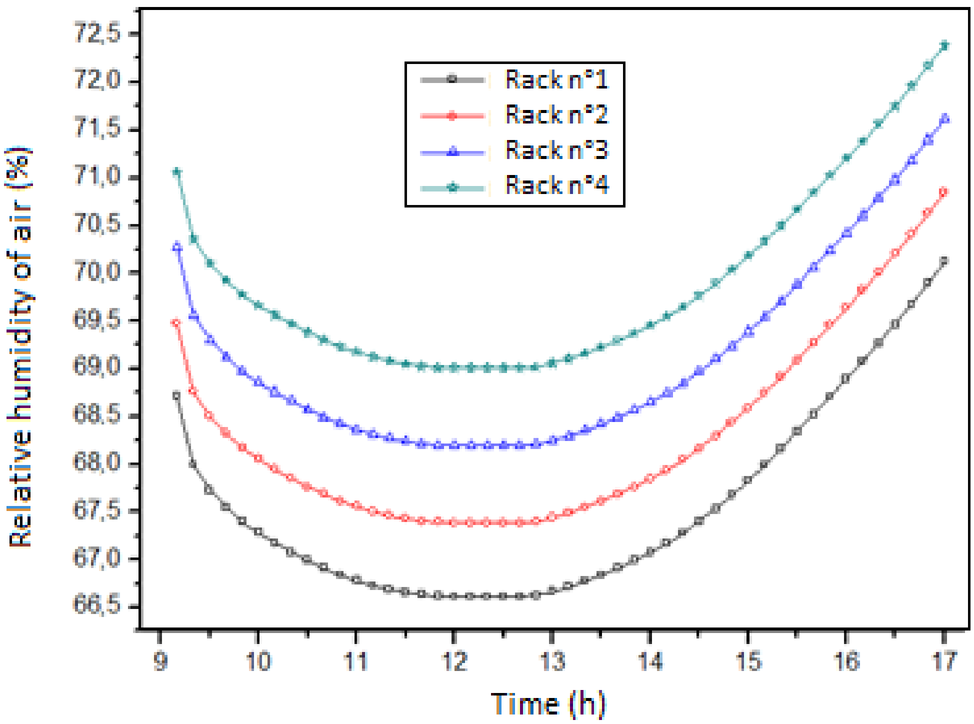

Figure 5:- Variation of the relative humidity of the air as a function of time.

The relative humidity of the air arriving at the level of the rack n°1 varies with the weather. It decreases from 68.71% to 66.61% between 9h and 12h 40min then increases to reach a value of 70.12% at 5h. At the same times, the relative humidity of the drying air increases as the air passes through the racks containing the okra out of the chamber. This means that the drying air becomes charged with moisture when it passes through a hurdle containing okra. The difference in the relative humidity of the air flowing through two consecutive trays ranges from 0.57% to 0.91%. Thus at 12h 40min, the air has a humidity of 66.61% at the level of the basket n˚1 against a humidity of 69.01% at the level of the basket n˚4.

Water content of okra at the level of the racks

The curve of the water content of okra at the level of each screen is represented by Figure 6. They are obtained by a polynomial adjustment of degree 4, of the experimental curves of the water contents of okra. These moisture content values were entered into the computer code to simulate the variation in the temperature of okra slices described previously, as well as the relative air humidity and drying kinetics of okra.

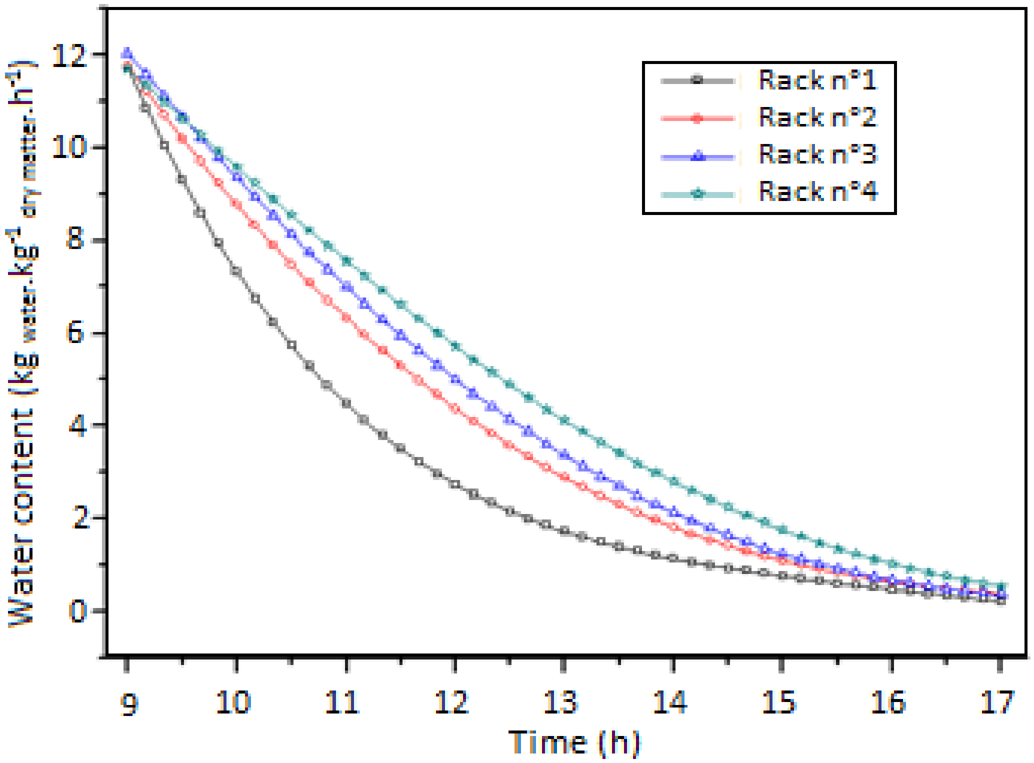

Figure 6:- Variation of water content as a function of time.

Drying kinetics of okra at the level of the racks

The drying speed or kinetics during the drying time is given in figure 7.

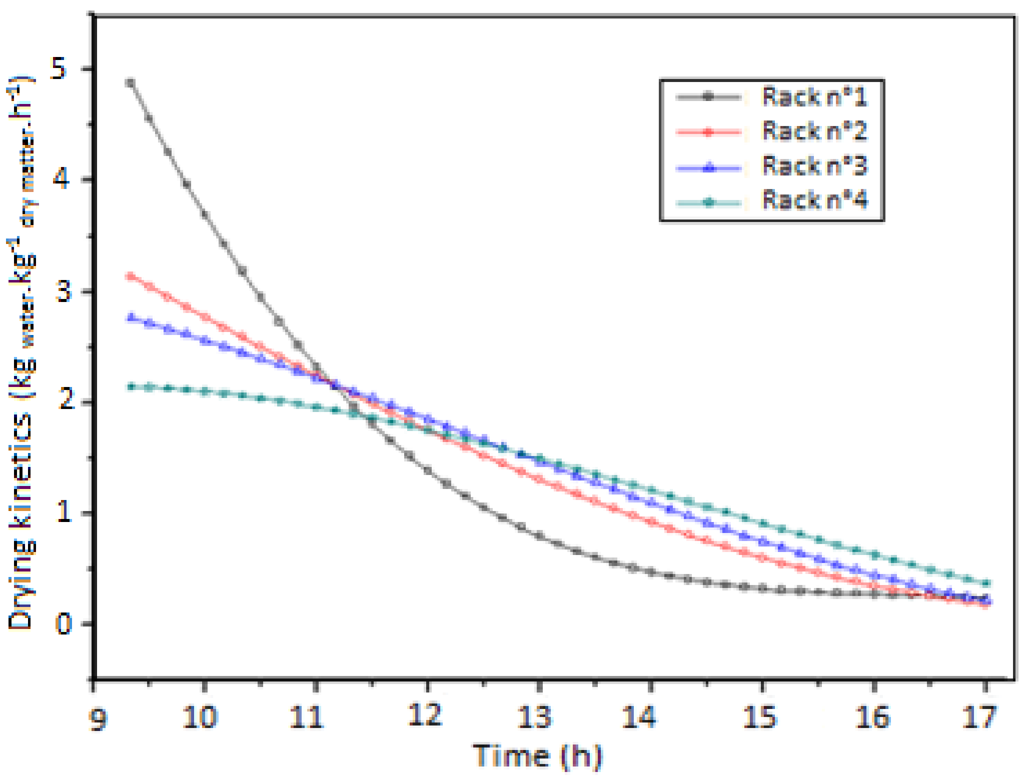

Figure 7:- Variation of the drying kinetics as a function of time.

We only observe the drying phase at decreasing speed on each curve. Between 9 a.m. and 11 a.m., the drying speeds of the okra from the first rack are higher than those of the racks n°2, n˚3 and n˚4. This explains why the okra in tray 1 released more water than that in the other trays. After 11h, we observe that the drying speeds of okra from rack n°4 are greater than those of okra from rack n˚3 to rack n°1 by decreasing values. This shows that the transfer of moisture in okra placed on racks n°3 and n°4 is faster than that in okra exposed on racks n°1 and n°2. If the drying time were prolonged, the drying speeds would tend to cancel out as the humidity of the product to be extracted will become minimal. The values of the drying speeds obtained at the start (9h) and at the end (17h) of a simulation day are recorded in Table 1.

Table 1:- Variation of the theoretical drying speed for one day of drying.

Product	Drying speed ($kg_{water}.kg^{-1}_{dry\ matter}.h^{-1}$)	
	Start of the day (9h)	End of the day (17h)
Okra of rack n°1	4.88	0.239
Okra of rack n°2	3.13	0.185
Okra of rack n°3	2.76	0.216
Okra of rack n°4	2.14	0.374

Figure 8 presents the experimental and theoretical drying kinetics of okra.

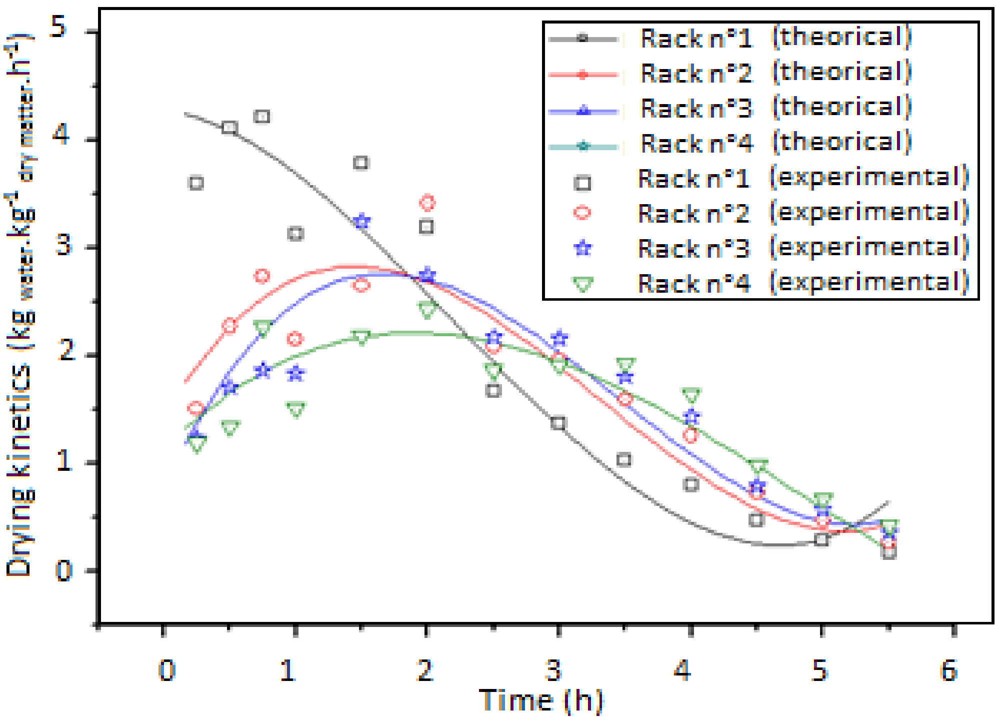

Figure 8:- Comparison of experimental and theoretical drying kinetics.

The experimental drying kinetics curves show two drying phases, which are the okra temperature phase and the decreasing speed phase. The theoretical drying kinetics curves at the level of the last three racks show the same drying phases except that of the first rack which only exhibits the phase of decreasing speed. In fact, the product warming up phase is a phase that takes place very quickly over a period of time for certain agricultural products but not for the vast majority of products [14]. This explains its inexistence on the figure of the theoretical drying kinetics at the level of the rack 1.

Conclusion:-

The simulation of the drying process allowed us to assess the variations in temperature of the okra slices placed on each rack and the variation in the relative humidity of the drying air in the chamber to be dried. The maximum temperature difference between a slice of okra located on racks n˚1 and n˚2 is 1.17˚C with a humidity difference of

0.91%. The theoretical drying kinetics curves at the level of the last three racks show the same drying phases. At the level of the first rack, only the phase of decreasing speed is observed. The values of the drying speeds obtained after 8 hours of drying (from 9 a.m. to 5 p.m.) are respectively 0.239 kg; 0.185 kg; 0.216 kg and 0.374 kg of water kg dry matter h^{-1} for rack n˚1 to n˚4.

References:-

[1] T. S. M. Ky, D. A. A. Traore, B. M. Pakouzou, B. Dianda, E. Ouedraogo and D. J. Bathiebo, Experimental Study of an Indirect Solar DryerUsing a New Collector System; Application to Mango and Ginger Drying, Contemporary Engineering Sciences, 14(1), 73 - 89, 2021.
[2] P. Udomkun, S. Romuli, S. Schock et al., Review of solar dryers for agricultural products in Asia and Africa: An innovation landscape approach, Journal of Environmental Management, 268:110730, 2020.
[3] S. Kam, G. W. P. Ouedraogo, B. Kaboré , B. M. Pakouzou, M. Ousmane and D. J. Bathiébo, Analysis of Tomato Drying by Using a Solar Tower Dryer in Natural Convection, Asian Journal of Physical and Chemical Sciences 4(2): 1-8, 2017.
[4] Y. B. Chauhan and P. P. Rathod, A Comprehensive Review on Solar Dryer, International Journal of Ambient Energy, 41(1):1-28, 2018.
[5] A. Kumar, R. Singh, O. Prakash and Ashutosh, Review on Global Solar Drying Status. AgricEngInt: CIGR Journal, 16(4), 161-177, 2014.
[6] R. Daghigh, R. Shahidian, H. Oramipoor, A multistate investigation of a solar dryer coupled with photovoltaic thermal collector and evacuated tube collector, Solar Energy, 199, 694-703, 2020.
[7] Y. Mohana, R. Mohanapriya, T. Anukiruthika, K. S. Yoha, J. A. Moses, C. Anandharamakrishnan, Solar dryers for food applications: Concepts, designs, and recent advances, Solar Energy, 208, 321-344, 2020.
[8] W. Pantaleo Missana, E. Park, and T. T. Kivevele, Thermal Performance Analysis of Solar Dryer Integrated with Heat Energy Storage System and a Low-Cost Parabolic Solar Dish Concentrator for Food Preservation, Journal of Energy, Article ID 9205283, 10 pages, 2020.
[9] A. Chavan, V. Vitankar, A. Mujumdar and B. Thorat, Natural convection and direct type (NCDT) solar dryers: a review, Drying Technology, 39, 1969-1990, 2020
[10] G. W. P. Ouedraogo, S. Kam, M. Sougoti, O. Moctar and D. J. Bathiebo, Numerical and Experimental Study of Natural Convection Air Flow in a Solar Tower Dryer, International Journal of Advanced Engineering Research and Science (IJAERS), 4(5), 2017.
[11] A. Midilli and H. Kucuk, Mathematical modeling of thin layer drying of pistachio by using solar energy, Energy conversion and management, 44, 1111-1122, 2003.
[12] T. Hadibi, A. Boubekri, D. Mennouche, A. Benhamza, N. Abdenouri, 3E analysis and mathematical modelling of garlic drying process in a hybrid solar-electric dryer, Renewable Energy, 170, 1052-1069, 2021.
[13] S. Vijayana, T. V. Arjunana and A. Kumar, Mathematical modeling and performance analysis of thin layer drying of bitter gourd in sensible storage based indirect solar dryer, Innovative Food Science and Emerging Technologies, 36, 59-67, 2016.
[14] M. Daguenet, les séchoirs solaires : théorie et pratique, Unesco, ISBN : 923202375X, 9789232023759, 578 pages, 1985.
[15] R. A. Okedun and E. A. Ajav Specific Heat and Thermal Diffissivity of Okra as affected by Moisture Content and Bulk density, Journal of Engineering and Applied Sciences, 2(12), 1729 - 1734, 2007.
[16] B. Dianda, 'Etude expérimentale et théorique du séchage convectif de la tomate en couche minces.', thèse de doctorat de l'université de Ouaga I Pr Joseph KI-ZERBO, 2016.